Applied Surface Science 673 (2024) 160894

Contents lists available at ScienceDirect

Applied Surface Science

journal homepage: www.elsevier.com/locate/apsusc

Full Length Article

The catalytic activity of metal–organic frameworks (MOFs) and post-synthetic modified MOF towards depolymerisation of polycarbonate

Patrycja Jutrzenka Trzebiatowska [a,*], Zofia Maramorosz [a], Mateusz A. Baluk [a], Maria Gazda [b], Arantxa Eceiza [c], Adriana Zaleska-Medynska [a]

[a] Department of Environmental Technology, Faculty of Chemistry, University of Gdansk, Wita Stwosza 63, 80-308 Gdańsk, Poland
[b] Institute of Nanotechnology and Materials Engineering, Faculty of Applied Physics and Mathematics, Gdansk University of Technology, Gabriela Narutowicza 11/12, 80-233 Gdańsk, Poland
[c] Group 'Materials+Technologies', Department of Chemical and Environmental Engineering, Polytechnic School, University of the Basque Country, Plaza Europa 1, Donostia-San Sebastián 20018, Spain

ARTICLE INFO

Keywords:
MOFs
Catalysis
Post-synthetic modification
Polycarbonate depolymerization
Chemical recycling
Bisphenol-A

ABSTRACT

Chemical recycling of polycarbonate (PC) recovers valuable chemicals like monomers but often requires catalysts for mild reaction conditions and high conversion rates. This study explores the use of metal–organic frameworks (MOFs) as catalysts for PC methanolysis. We investigated the catalytic activity of amine-containing MOFs, specifically ZIF-8, MAF-6, and UiO-66-NH_2, which have basic active sites favouring PC depolymerisation. MOFs were characterised using X-ray diffraction (XRD), Fourier-transform infrared spectroscopy (FTIR), scanning electron microscopy (SEM), and Brunauer–Emmett–Teller (BET) analysis. We examined the effects of temperature, catalyst content, and time on PC recycling efficiency and also conducted post-synthetic modification (PSM) of MOF-5 to assess its catalytic performance in PC depolymerisation. Methanolysis yielded bisphenol A (BPA) and dimethyl carbonate (DMC), with conversion rates confirmed by nuclear magnetic resonance (NMR). MOF catalysts significantly enhanced conversion rates compared to reactions without catalysts, with ZIF-8 and MAF-6 achieving nearly 100% PC conversion. PSM of MOF-5 with ethylenediamine (ED) led to increased PC conversion. Additionally, the MOF-based catalysts were recovered and reused for up to three cycles.

1. Introduction

Chemical recycling of plastic waste draws the researchers' attention and gains more significance as being complementary to mechanical recycling [1,2]. This method enables the depolymerisation of waste that cannot be processed by simple mechanical operations or would otherwise be incinerated or landfilled due to quality loss. From recovered raw materials, including monomers, dimers or smaller organic fractions, polymers of similar quality can be obtained in traditional installations, as virgin polymers produced from monomers obtained from oil or gas [3]. This preserves natural resources and is a step towards closing the loop [4].

One of the commonly used polymers is polycarbonate (PC) which contains in the chain the repeated structural unit of the carbonate type [–O–CO–O–]. The global demand for PC was estimated at 4.5 million tons in 2022 as published by Statista Research Department [5]. PC is widely used as material for safety glazing (i.e. bullet-proof structures), dentures, food packages, electrical components, and compact disks (records and data disks) due to its properties such as high impact strength, good heat resistance, low water absorption, good electrical properties and transparency [6,7]. However, the production of PC involves the use of phosgene and the release of harmful chemicals such as vinyl chloride, dioxins, benzene, bisphenol A (BPA), and formaldehyde, raising significant environmental concerns. Moreover, bisphenol A and its derivatives have been a topic of concern regarding their potential toxicity since BPA is a known endocrine disruptor [8]. Therefore focusing on the recycling of PC is beneficial from an environmental point of view, given its slow degradation rate and persistence in the environment [7,9]. Nevertheless, mechanical recycling has limitations in terms of the quality and purity of recycled polymer due to the deterioration of mechanical properties and partial degradation of the material. Hence, the chemical recycling of PC is broadly studied [10–13], including pyrolysis[14], cracking or solvolysis (mainly methanolysis [15], glycolysis[16] and hydrolysis[17]). These processes can yield

* Corresponding author.
E-mail address: patrycja.jutrzenka-trzebiatowska@ug.edu.pl (P. Jutrzenka Trzebiatowska).

https://doi.org/10.1016/j.apsusc.2024.160894
Received 14 June 2024; Received in revised form 26 July 2024; Accepted 1 August 2024
Available online 2 August 2024

starting monomers (BPA and dimethyl carbonate, DMC) or valuable intermediates. Due to the poor solubility of PC in methanol, alcoholysis is carried out at high temperatures and pressure, often requiring additional organic solvents, harsh pH conditions[11] and the presence of a catalyst, e.g. earth metal oxides [18,19], deep eutectic solvent based on choline chloride [20] or nanoparticles [19,21]. Table 1 presents a comparison of BPA yields obtained by different heterogenous catalysts employed for PC methanolysis. Solid basic catalysts are highly required in sustainable chemistry due to their higher efficiency in reactions, recyclability and thus process simplification and volume waste reduction [22]. An interesting concept is to use a metal–organic framework (MOF) as a depolymerisation catalyst [23]. MOFs such as ZIF-8, ZIF-67 and MOF-5 [24], bimetallic MOF-74 (Mg/Mn) [25] or MOFs composites of $CoFe_2O_4$@ZIF-8/ZIF-67 [26] were used as catalysts for PET depolymerisation.

Metal-organic frameworks are crystalline materials composed of metal nodes and organic linkers [27]. MOFs were investigated regarding catalytic applications as they offer several advantages over traditional catalysts, such as stability in various conditions, selectivity towards specific products due to their pore structure, reusability, high surface area providing a large number of active sites, and tunability since they can be functionalised with functional groups or nanoparticles [28,29]. The latter feature is desirable, when pristine MOFs employed as catalysts are not efficient, due to the lack of coordination positions for substrate binding. Therefore, the functionalisation, direct or post-synthetic treatment introducing groups as acid or base centres (e.g. $–SO_3H$, $–NH_2$, of inorganic nodes or organic linkers can enhance catalytic properties [30,31]. This allows for promoting many reactions e.g. hydrolysis, dehydration, isomerisation, condensation [27].

In this work, for the first time we demonstrate the possibility of using pristine MOFs and modified by post-synthetic modification (PSM) as catalysts for the depolymerisation of PC in a methanolysis reaction. To our knowledge, no reports in the recent literature have explored these approaches for PC chemical recycling. We selected MOFs with amine groups in their structures, as methanolysis achieves higher yields in a basic environment [9]. The chosen MOFs, such as ZIF-8 and MAF-6 possess surface N-moieties and OH groups, which can act as basic active sites particularly interesting for the combined activation of alcohols and esters [32]. Also, UiO-66-NH_2, compared to its analogue UiO-66, exhibits higher activity and selectivity in many organic reactions [33]. Moreover, PSM aimed to introduce amine groups to boost the depolymerisation efficiency of MOF-5. All samples were characterised in terms of morphologies, structural and surface properties and use in a model PC methanolysis reaction with varying process conditions.

Table 1
Comparison of results with other studies in the literature.

Catalyst	Reaction conditions			BPA yield (%)	Reference
Name	T (°C)	t (h)	Amount of used reagents: m(Cat):m(PC) n(MeOH):n (PC) m(solvent):m (PC)		
CeO_2-CaO-ZrO_2	100	2	0.05:1 6:1 –	95.8	[57]
TBD-functionalised silica gel (Si-TBD)	65	2.5	0.32:1 13:1 –	88	[58]
CaO/MCF	125	2.5	0.016:1 8:1 2:1 (THF)	96	[59]
$NaAlO_2$	60	2	0.04:1 13:1 2:1 (THF)	96.8	[15]
15 % CaO/Ce-SBA-15	130	3	0.3:1 10:1 1.5:1 (THF)	94.5	[60]
Ca-Al_2O_3	130	3	0.03:1 8:1 1.5:1 (THF)	96.3	[61]
[Bmim][Cl]	105	2.5	1:1 12:1 –	95.5	[62]
ZIF-8	130	3	0.05:1 8:1 2:1 (THF)	94.1	This work
MOF-5-ED	130	3	0.05:1 8:1 2:1 (THF)	99.2	This work

2. Materials and methods

2.1. Synthesis of MOF-based catalysts

UiO-66-NH_2: $ZrCl_4$ (1.715 mmol; supplied by Thermo Scientific) and 2-aminoterephthalic acid (1.715 mmol; supplied by Sigma Aldrich) and modulator-acetic acid (0.05 mol; supplied by Chempur) were sonicated in 100 ml N,N-dimethylformamide (DMF, supplied by Avantor Performance Materials). Then distilled H_2O was added. The reaction took place at 120 °C for 24 h. The mixture was centrifuged, washed with DMF, then methanol and dried at 60 °C [34].

ZIF-8: $Zn(NO_3)_2{\cdot}6H_2O$ (10 mmol; supplied by Eurochem) was dissolved in 100 ml of methanol (supplied by Avantor Performance Materials) and then a solution of 2-methylimidazole (40 mmol; supplied by Sigma Aldrich) in 100 ml of methanol was slowly added. The mixture was stirred for 24 h at room temperature. Then, the solid was centrifuged, washed with methanol (supplied by Stanlab) and dried at 60 °C [35].

MAF-6: The concentrated aqueous ammonia solution (25 % NH_4OH, 40 ml; supplied by Avantor Performance Materials) of ZnO (2 mmol; supplied by Avantor Performance Materials) was added slowly into a methanol (30 ml) and cyclohexane (6.66 % v/v; supplied by Chempur) solution of 2-ethylimidazole (4 mmol; supplied by Sigma Aldrich) and stirred at room temperature for 0.5 h. After the synthesis, the obtained solid was collected by centrifugation and washed with methanol, repeated three times. The powder was dried under a vacuum [36].

MOF-5: $Zn(NO_3)_2{\cdot}6H_2O$ (2.4 g, 8.1 mmol) and terephthalic acid (0.66 g, 3.97 mmol; supplied by Acros Organics) were dissolved in 80 ml of DMF (80 ml). To the solution was added dropwise 1.5 ml (16 mmol) of pure triethylamine (supplied by Avantor Performance Materials) at room temperature, which allowed rapid crystal growth in ambient reaction conditions. The mixture was stirred for 90 min and the white solid was centrifuged, washed three times with DMF and then immersed in chloroform for 3 days with fresh chloroform (supplied by Avantor Performance Materials) added every 24 h for its activation. The powder was dried under vacuum at 70 °C [37].

2.2. Post-synthetic modification of MOF-5

MOF-5-ED: Pure MOF-5 (768 mg, 1 mmol), dehydrated at 150 °C for 12 h, was suspended in anhydrous toluene (30 ml; supplied by Sigma Aldrich) and then ethylenediamine (ED, 360 mg, 6 mmol; supplied by Chempur) was added. The mixture was stirred with heating to reflux (ca.150 °C) for 24 h under nitrogen. The formed solid (MOF-5-ED) was centrifuged, washed with anhydrous toluene and dried at 100 °C under a vacuum [37].

2.3. Characterisation of MOFs

Powder X-ray diffraction (pXRD) measurements were investigated on a Philips X'PertPro MPD (Almelo, The Netherlands) with Cu Kα radiation (λ = 1.5418 Å). X-ray diffractograms were collected at 2θ angle from 5° to 60° to determine the crystal structure of the MOF samples.

The morphology, shape and size were observed using a scanning electron microscope (SEM, JEOL JSM-7610F Tokyo, Japan). The Fourier-transform infrared (FTIR) spectra measurement was performed with the KBr pellet technique using a Nicolet iS5 Fourier spectrometer (Thermo Scientific) in absorbance mode. The spectra were obtained after 64 scans in a range from 4000 to 500 cm^{-1} with a resolution of 4 cm^{-1}. The Brunauer–Emmett–Teller (BET) surface areas of the obtained samples were determined using a 3P Instrument Micro 200 sorption analyser. All samples were degassed at 200 °C for 5 h prior to nitrogen adsorption measurements. The BET surface areas were evaluated by the multipoint BET method using adsorption data for the relative pressure (P/P_0) range of 0.005–0.1. The external surface areas (S_{ext}) were determined by the *t-plot* method for the relative pressure range of 3.5–6.0 The pore size distribution was calculated using the Horvath-Kawazoe / Saito-Foley (HK/SF) and density functional theory (DTF) methods, for comparison. The thermogravimetric analyses (TG) were performed on TGA/STDA 851 Mettler Toledo and TGA 8000 Perkin Elmer equipments to evaluate the thermal stability of MOFs. Samples were heated from room temperature to 800 °C at a heating rate of 10 °C min^{-1} under a nitrogen atmosphere.

2.4. Procedure for methanolysis of PC in the MOFs presence

Weighted amounts of PC granules of size 2x2x4 mm (2 g; W_{PC}; supplied by SABIC Lexan), catalyst (5 wt% of PC; W_{cat}), methanol (nMeOH:nPC=8:1) and tetrahydrofuran, THF (mTHF:mPC=2:1; supplied by Chempur) were added into an Teflon lined steel autoclave of 100 ml volume. The mixture was heated up in the oven to the given temperature (110, 120 or 130 °C) and maintained for a certain time (1, 2, or 3 h) at autogenous pressure. The resulting mixture was filtered using filter paper (W_f) and then the remaining solid residue was dried and weighted (W_p, filter paper, un-reacted PC and catalyst). The filtrate was distilled to remove unreacted methanol, THF and DMC, and the residue (monomer) in the flask was recrystallised with water. The mixture was filtered and dried to obtain bisphenol-A (W_{BPA}). Methanolysis conversion of PC and yield of BPA were calculated by the following equations (Eq1-Eq2):

$$Conversion\ of\ PC = \frac{W_{PC} - (W_p - W_f - W_{cat})}{W_{PC}} \bullet 100\% \quad (1)$$

$$Yield\ of\ BPA = \frac{W_{BPA}}{W_{PC}} \bullet \frac{M_{PC}}{M_{BPA}} \bullet 100\% \quad (2)$$

where: M_{PC}=254.3 g/mol; M_{BPA}=228.3 g/mol.

In order to explore the catalyst activity, two additional methanolysis runs were carried out, namely, *1)* catalytic test on a larger scale, where PC amounted to 10 g and *2)* depolymerisation on the real plastic sample, PC originated from laboratory safety glasses cut into 10x10x2 mm pieces.

Nuclear Magnetic Resonance (^{1}HNMR) spectra of the reaction mixture were recorded with a Bruker AV III 700 MH spectrometer at ambient temperature. Samples were dissolved in $CDCl_3$ solvent and DMF was used as the internal standard. Monomer, BPA, was also characterised via the FTIR technique, described above.

3. Results & discussion

3.1. Metal-organic frameworks characterisation

Fig. 1 presents the structural, thermal properties and morphology of synthesised MOFs. The results of the pXRD analysis (Fig. 1a) show that the diffractograms exhibit high-intensity reflections which indicate the

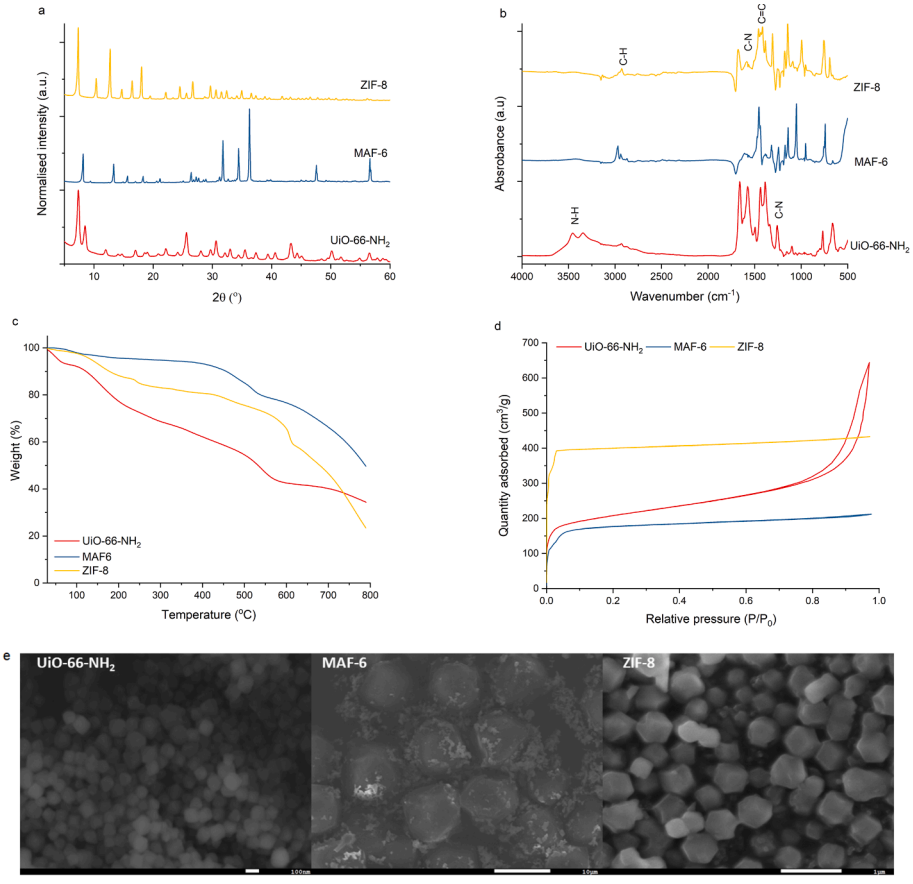

Fig. 1. MOFs characterisation: a) XRD, b) FTIR, c) TGA, d) BET adsorption–desorption isotherm and e) SEM of prepared catalysts.

high crystallinity of MOFs. In addition, pXRD patterns of the MOFs, are all similar to the XRD patterns reported in the literature [34–36]. UiO-66-NH_2 exhibits less sharp peaks however, the patterns match the main typical peaks at 2θ angle. For UiO-66-NH_2 the original peaks are at 7.4°, 8.5°, 12.0° and 25.6°. The diffraction peaks of ZIF-8 appear at 2θ values of 7.35°, 10.52°, 12.73°, 14.71°, 16.45 and 18.03°. This pattern goes well with the standard of ZIF-8. MAF-6 exhibits following peaks at 2θ 8.18°, 13.35°, 15.67° and 18.29°. Signals at the 2θ angle of 31.22° and 34.44° can result from impurities, such as a linker in the pore structure.

The FTIR spectra of all prepared MOFs are presented in Fig. 1b. For UiO-66-NH_2, two absorption bands can be found at 3350 cm^{-1} and 3451 cm^{-1} as a result of asymmetric and symmetric stretching vibrations of a primary amino group (–NH_2) [38]. Also, the C-N bonding is observed at 1255 cm^{-1} and 1382 cm^{-1}, and the peak at 1656 cm^{-1} can be assigned as the bending vibration of N–H. Two strong absorption bands in the region of 1560–1700 cm^{-1} and 1380–1415 cm^{-1} are attributed to carboxylate asymmetric and symmetric stretching coming from terephthalic acid. ZIF-8 and MAF-6 show similar spectra, as they possess imidazole rings. In the region 2900–2930 cm^{-1}, ZIF-8 exhibits one band assigned to the methyl group while MAF-6 shows two bands corresponding to the methyl and methylene groups. Also, there can be found C–N bond stretching (1586 cm^{-1}), C–C stretching vibration of imidazole ring (1454 cm^{-1}) and several bands in the range of 1170–900 cm^{-1} can be ascribed to the in-plane bending signals of the imidazole ring, consistent with their vibrations reported in the literature [35,39,40].

The results of the TG analysis are displayed in Fig. 1c. All MOFs show up to 450–550 °C several weight loss steps, which can be attributed to different processes, such as moisture removal, evaporation of the solvents encapsulated in the MOF cages and/or degradation of their organic constituents. The mass evolution observed above this temperature interval is mainly related to their inorganic constituents, with a sharp decrease in weight around 450–500 °C indicating total degradation of the structure. MAF-6 is the most stable, since except a moisture-related mass loss, it shows only one degradation step around 400 °C. ZIF-8 and UiO-66-NH_2 show mass loss due to the vaporisation of water and solvents removal which were capped in the MOF cages, before the degradation of their organic components [41]. All MOFs show high residue content attributed to the inorganic components.

The results of surface area measurements of the samples can be found in Table A1. The BET surface areas for UiO-66-NH_2, ZIF-8, and MAF-6, as measured, are 768, 1601, and 306 m^2g^{-1}, respectively. The estimated pore sizes are 0.51, 0.50, and 0.41 nm for UiO-66-NH_2, ZIF-8, and MAF-6, respectively. The porosity of UiO-66-NH_2 and ZIF-8 is similar to other comparable materials found in the literature [41–43]. However, prepared MAF-6 exhibits a much lower specific surface area as suggested in the literature [44,45]. It could be a consequence of pore blockage by used solvents. Fig. 1d presents the BET adsorption–desorption plots. The isotherm of these MOFs, according to BET, aligns with type I isotherms. The degree of nitrogen adsorption initially increased, reaching saturation at ~ 0.06, ~0.05 and ~ 0.07p/p_0, and eventually reaching a gas saturation point of ~ 205, ~394 and ~ 162 cm^3g^{-1} for UiO-66-NH_2, ZIF-8 and MAF 6, respectively.

The morphology of the MOFs was studied by SEM. ZIF-8 exhibits a polyhedral morphology with a particle size of about 400 nm. The obtained MAF-6 has the shape of polyhedrons with a size of 8–10 μm. Bright spots on the part surface may be from unreacted reagents. UiO-66-NH_2 forms polyhedral shapes with small sizes around 90 nm. The obtained crystal microstructures are in agreement with the literature [32,46,47].

3.2. Methanolysis of PC in the presence of MOF-based catalysts

Fig. 2 illustrates the conversions of PC and the yields of BPA recovered during methanolysis under different reaction temperatures (110, 120 and 130 °C) and with various MOFs employed as catalysts. The

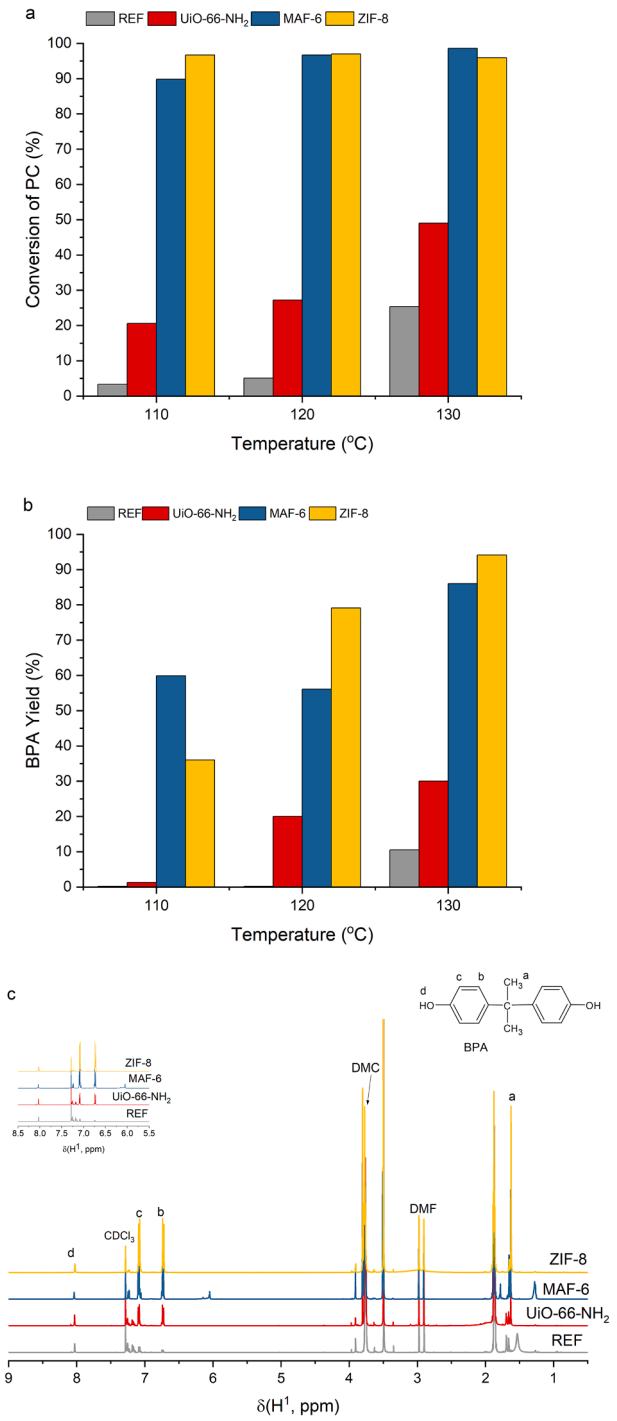

Fig. 2. Conversion of PC (a) and BPA yield (b) in the presence of MOFs at various reaction temperatures, c) NMR of the post-methanolysis reaction mixture.

reference sample (REF) represents the reaction conducted without any catalyst. As evident from the graph, increasing the reaction temperature enhances both, the conversion rate and the BPA yield for all samples. In the case of the REF sample, the conversion rate rises from 3 % to 25 %, while the BPA yield increases from 0.2 % to 10 %. The utilisation of MOFs enables higher conversion rates compared to those in the absence of catalysts. Notably, ZIF-8 and MAF-6 exhibit the highest catalytic activity, achieving approximately 90 – 100 % PC conversion, while the BPA yields increase at higher temperatures ranging from 36 to 94 % and 59 to 89 %, respectively. This suggests that despite achieving complete

conversion of PC, additional energy is required to convert all smaller compounds into monomers. The obtained values for PC conversions and BPA yields are comparable to those presented in the literature under similar methanolysis conditions as shown in Table 1. Both, catalysts are composed of Zn^{2+} as a metal centre and imidazole rings, where the active site from −N- moiety plays a role in the catalysis [33]. The better performance of ZIF-8 over MAF-6 in PC depolymerisation can be partially attributed to its morphology (Table A1), as previous studies have indicated that catalysts with smaller particle sizes (ZIF-8, ca. 432 nm) tend to exhibit higher activity than larger crystals (MAF-6, ca. 9.9 μm) [48]. The reaction probably takes place on the external surface of the ZIF-8 and MAF-6 crystals, where active basic nitrogen atoms are located. At 130 °C, UiO-66-NH_2 reaches 49 % of the conversion rate and 30 % BPA yield. Even though UiO-66-NH_2 is recognised as a highly active catalyst, these values are relatively low and can be attributed to restricted mass transfer between PC pellets (solid) and fine particles of UiO-66-NH_2 (ca. 90 nm) and less exposed Zr sites [49]. Also, the activity of the basic sites in the MOF plays a role in its performance. As listed in Table A1, the basic site for UiO-66-NH_2 is aromatic amine (Ar-NH_2) which is less basic than imidazole (p*K*a 4.63 and 6.95, respectively) [50]. Moreover, in the methanolysis of PC catalysed by MOFs, the part of catalytic sites likely becomes obstructed by degradation products formed during PC depolymerisation, such as oligomers and dimers, hence such microporous MOFs as UiO-66-NH_2 and characterised by nanosized particles (ca. 90 nm) a have difficulty for catalysing reaction involving bulky molecules due to rising diffusion limitations and agglomeration [33]. Consequently, the conversion of PC into monomers mainly occurs at the MOF surface rather than within the pores, similar to the other transesterification reactions [51]. This phenomenon is directly connected to the PC depolymerisation mechanism (Scheme 1), which involves the following main steps: *(I)* swelling of PC pellets due to solvent penetration and random scission into solid oligomers, *(II)* size reduction caused by dissolution of the solid oligomer, *(III)* the conversion from dissolved oligomers into monomers, BPA and DMC, as described in detail by Kim et al.[52]. Methanol together with THF acting as a co-solvent soften the PC pellets and facilitates the methanol penetration into polymer cracks. The use of catalysts clearly enhances the reaction compared to the reference sample. The possible depolymerisation mechanism in the presence of a catalyst can be based on the activation of the nucleophile by MOF, which consists of both active basic and acid sites. Strong basic sites in ZIF-8 and MAF-6 (−N−moiety) or aromatic amine in UiO-66-NH_2 interact with the hydrogen of the hydroxyl group in CH_3OH, weakening or breaking the O–H bond to create a negative charge on − OH or to form alcoholate ion, CH_3O−,

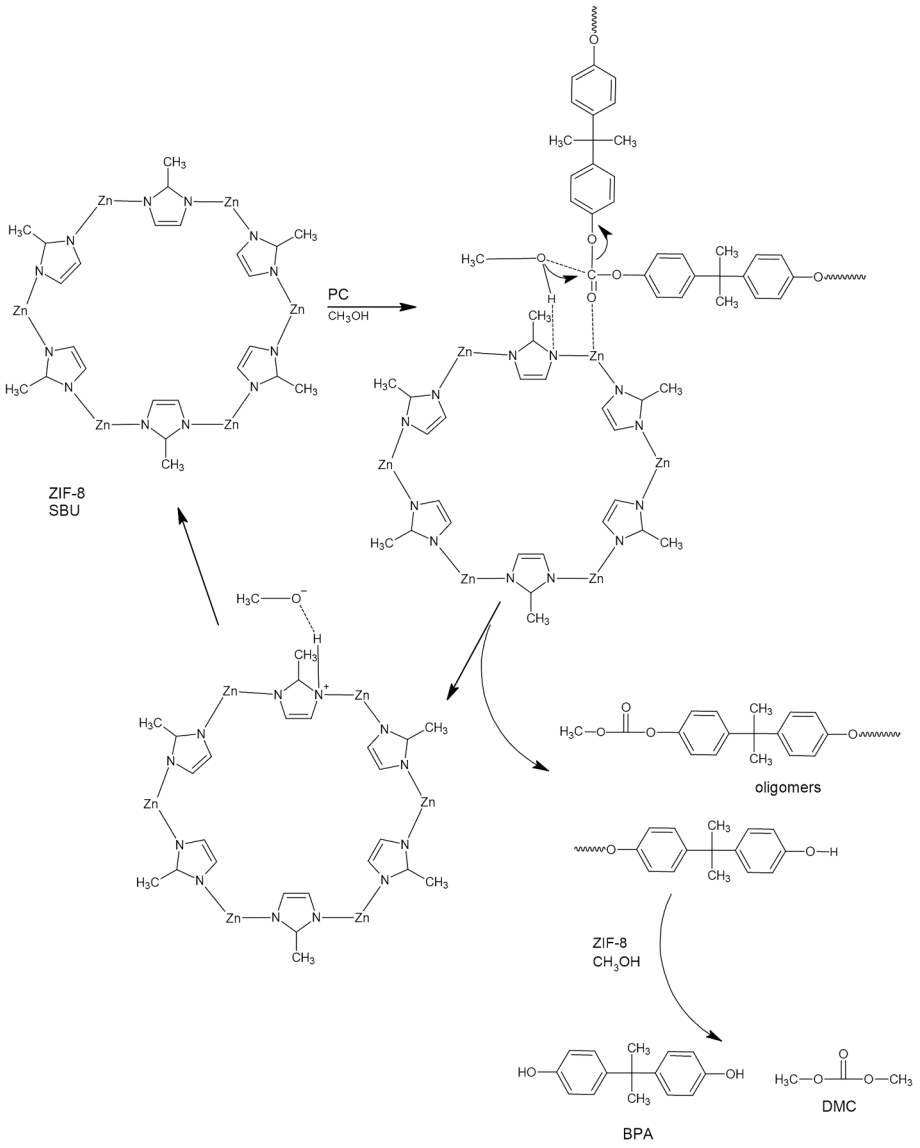

Scheme 1. Methanolysis of polycarbonate in the presence of ZIF-8.

respectively. As a nucleophile, CH_3O- attacks the carbonyl carbon atom in the ester group of the polymer. This is also facilitated by an acid site from MOF (metal centre, Zn^{2+} or $Zr^{4+)}$ that interacts with the lone pair electrons of the oxygen atom of the carbonyl group in PC. The long-chain PC is continuously broken into short chains and the molecular weight becomes smaller. Then, these short-chain PC react with methanol catalysed by MOF to generate oligomers, and dimers and finally to obtain the products BPA and DMC [18,33,53].

Given the high catalytic activity of ZIF-8 among the tested MOFs, its efficiency was tested in additional depolymerisation runs. In these reactions, *1)* the amount of PC pellets was increased fivefold, and *2)* a waste sample was tested, with PC derived from laboratory safety glasses, cut into small pieces. Methanolysis was carried out under the same procedure with the following conditions 5 % wt. catalyst, 130 °C, 3 h, only for reaction on a larger scale using a 200 ml volume autoclave. The achieved PC conversions were respectively 87.5 and 91.5 %, and yields calculated by NMR 91.5 and 97.8 %, respectively (Table A2). This shows applicability of MOF-based catalysts both for larger scale and also for post-consumer waste.

In order to confirm the presence of BPA in the reaction mixture after the completion of the process, ^{1}HNMR analysis was performed. The NMR spectrum is shown in Fig. 2c. The formula of BPA is shown and labelled for easier identification of the molecule structure. The signal at δ 8.01 ppm is characteristic of the protons of the hydroxyl group (d). The peaks at δ 7.10–7.02 and δ 6.76–6.66 (c, b) ppm indicate the presence of aromatic protons of the benzene ring, while the one at δ 1.60 ppm indicates the presence of methylene protons (a). The obtained spectrum agrees well with that given in the literature [54]. The remaining peaks at the following chemical shifts: 7.26, 3.80 and 1.83, doublet 2.97 and 2.90 ppm are from solvents $CDCl_3$, THF, and DMF, respectively. The peak at the chemical shift of 3.77 ppm is from the second PC depolymerisation product, dimethyl carbonate [55,56]. In the NMR spectra of the samples obtained with various catalysts, we can clearly see the differences in the intensities of the peaks corresponding to BPA. In the case of ZIF-8 and MAF-6, where almost 100 % depolymerisation is achieved, the a, b and c peaks are of high intensity. When considering UiO-66-NH_2, the reaction took place only partially, the intensities are low and also peaks showing the presence of oligomers appear around 7.11–7.21 ppm and 7.21–7.30 ppm (inset of Fig. 2c), suggesting not completely depolymerised products. Fig. A1 shows FTIR spectra of the recovered monomer, BPA, from a methanolysis reaction catalysed by ZIF-8 as the confirmation of obtaining the wanted monomer. The broad peak of stretching vibrations from the O–H groups was observed at about 3330 cm^{-1}. At the wavenumber of 3030 cm^{-1}, a band corresponding to the stretching vibrations of the C–H groups of the aromatic ring was recorded. In the range below 1500 cm^{-1}, peaks of stretching vibrations of C-O and C–H single bonds were present.

3.3. Post-synthetic modification of MOF-5

The highest conversion of PC was found for the reactions with MOFs containing zinc metal (ZIF-8 and MAF-6), as a metal centre. Therefore, for further investigation, we synthesised MOF-5, which consists of zinc as a metal centre and terephthalic acid as ligands and then employed a simple PSM technique to functionalise MOF-5. Pristine MOF-5 has acidic properties and can act as a solid acid catalyst [63], however, MOF-5 has coordinatively unsaturated sites (CUSs) that can be altered via PSM to create a solid base. For this purpose ethylenediamine (ED) was chosen as the modifier which links one amine group to the CUS of Zn(II) in MOF-5, as reported in the study of Chen et al. 2014 [37]. As previously mentioned, base catalysts should promote the methanolysis reaction towards a higher conversion rate and monomer recovery.

The colour change in MOF crystals from white to light yellow indicated the effective grafting of ED onto MOF-5. Also, the amine grafting to MOF-5 was confirmed by FTIR, XRD and TGA (Fig. 3) by comparison with pristine MOF-5. In the FITR spectrum (Fig. 3a), the peaks in the range of 3400–3100 cm^{-1} correspond to N–H asymmetric and symmetric stretching vibrations, showing the presence of ED in MOF-5-ED. The XRD patterns of MOF-5 and MOF-5-ED (Fig. 3b) are qualitatively similar one to another indicating the preservation of crystallinity following the PSM process. However, some reflections differ in the intensities, e.g. those at 8.79° and 9.74° are very small in the MOF-5-ED pattern, while others are seen at lower or higher angles. The observed changes may be attributed to the presence of the ED groups which influence unit cell parameters. Diffraction peaks of MOF-5 appear at 2θ angles of 8.79°, 9.74°, 12.69°, 14.77°, 17.66 and 19.25°, while for MOF-5-ED at 12.03°, 13.84°, 15.98°, 18.26°, 22.35° and 23.36° can be seen. After the PSM with ED, no weight loss related to moisture or solvents

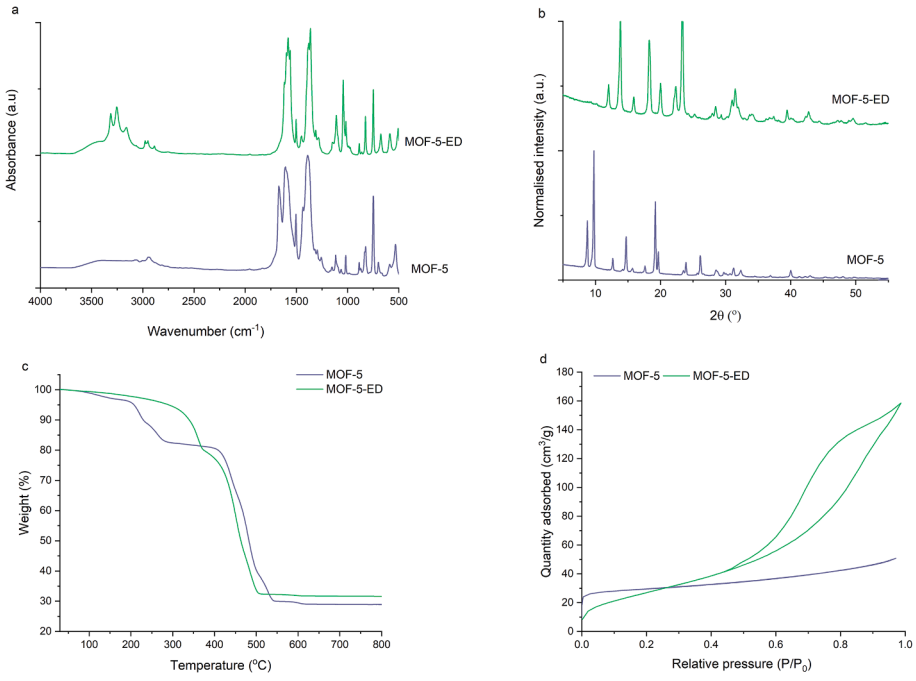

Fig. 3. Characterisation of MOF-5 before and after PSM with ethylenediamine (MOF-5-ED): a) FTIR, b) XRD, c) TGA and d) BET adsorption–desorption isotherm.

was observed, up to the mass loss occurring around 350 °C, which corresponds to the combustion of the organic linker (Fig. 3c). Moreover, no mass loss related to ED presence (boiling point 116 °C) was observed, confirming the successful attachment of the diamine to the parent MOF structure. However, the modification with ethylenediamine led to a decrease in specific surface area from 111 to 89 m^2g^{-1}, and a change in pore size from 0.45 to 0.82 nm (Table A1). In addition, the nitrogen adsorption–desorption isotherm changed in appearance from Type I for MOF-5 to Type II for MOF-5-ED (Fig. 3d) [64]. This is likely due to the bulky nature of ED, which could obstruct the pores of MOF-5 after grafting [65].

Pristine MOF-5 reaches low values of PC conversion (16.9 %) and BPA yield (34.5 %), therefore the effect of post-synthetic modification on the catalytic activity of the MOF-5 material was evaluated. Fig. 4 illustrates notable differences in PC conversion and monomer yield between the catalysts before and after PSM, across a range of temperatures (110–130 °C). The simple PSM of MOF-5 with ethylenediamine resulted in the desired outcomes and led to a significant enhancement in PC conversion (97.3 %) and increased yield (99.2 %) of the monomer compared to the unmodified MOF-5.

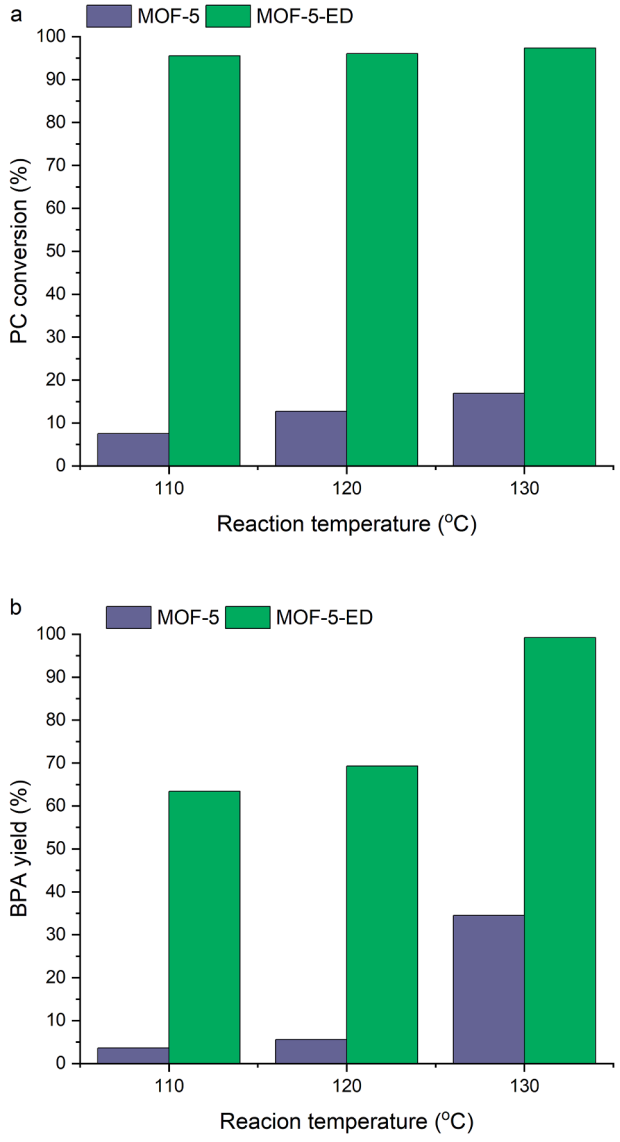

Fig. 4. Conversion of PC (a) and BPA yield (b) in the presence of MOF-5 and MOF-5-ED.

3.4. Influence of reaction parameters on methanolysis efficiency: Time and catalyst content

Considering that ZIF-8 and MOF-5-ED demonstrated the best performance in PC methanolysis, we investigated the effect of catalyst concentration and reaction time on PC recycling efficiency at the optimal reaction temperature of 130 °C (Fig. 5). It is evident that reaction time significantly influences PC conversion and subsequent BPA yield, even for the reference sample. Extending the reaction time is directly related to the mechanism of the depolymerisation, where the PC granule first is swelled and first cracks appeared in the polymer and activated nucleophile can attack the carbonyl bond to recover intermediates and finally the monomers. A longer reaction time ensures that the process will achieve complete depolymerisation. Within 1 h of reaction time, less than 10 % of BPA is recovered. Extending the reaction time to 2 h results in approx. 77 % PC conversion for MOF-5-ED and only 20 % for ZIF-8. However, when the reaction is extended to 3 h, nearly 100 % conversion of PC is achieved for both catalysts. MOF-5-ED exhibits higher PC conversions and yields than reaction with ZIF-8, even when lower temperatures are applied (Table A2). This may be caused by the presence of ED due to its basicity (p*K*a of ED at 0 °C=10.712) and high activity in this reaction.

When comparing the use of different catalyst amounts in the reaction, it is observed that for ZIF-8, there is no significant difference in PC conversion, with only a slight decrease in BPA yield. In contrast, for MOF-5-ED, higher catalyst content leads to higher BPA yield, rising from 61 % to 99 %, suggesting a positive correlation between catalyst amount and yield which may be a result of better access to active sites.

3.5. Recovery of the catalyst and reuse

In the presented work, the stability of MOFs in terms of catalytic activity was also examined. At the end of each methanolysis reaction, the MOF catalysts were separated from the reaction mixture by centrifugation (6000 rpm, 5 min). MOF-based catalysts were suspended in 20–30 ml of methanol and then stirred for 2–3 h at 60 °C. The solid MOF catalyst precipitate was then dried (60 °C, 24 h) and reused in the next PC methanolysis cycle at optimised conditions (130 °C, 3 h, 5 % of catalyst content in relation to PC). Fig. 6a and b show FTIR and XRD studies for a comparison between fresh (ZIF-8 and MOF-5-ED) and recovered catalysts (ZIF-8-rec and MOF-5-ED-rec). The FTIR spectra for the recovered samples do not show significant differences in the structure of the materials. Only the MOF-5-ED-rec catalyst, after recovery, shows new bands around 2800–3000 cm^{-1} that may indicate contamination of the sample with monomer residue. XRD revealed that each reaction run causes a loss in the crystallinity of ZIF-8 since the intensities of the main peaks decrease whereas their widths increase. However, the XRD patterns of the fresh and recovered ZIF-8 are almost the same (Fig. 6b). In the case of MOF-5-ED, the recovered catalyst shows minor changes in the structure, shifting towards rather to that of MOF-5 before PSM. Also, like in the FTIR spectrum, the broad peak around 20° is probably due to the presence of BPA in the pores of MOFs. BET analysis of both, ZIF-8-rec and MOF-5-ED-rec, showed lower specific surfaces than their initial structures (Table A1). The size and shape of crystals remained similar after the recovery, however, the particles tended to be more agglomerated (Figs A3 and A4).

The catalytic activity of the three MOF catalysts before and after reuse in the PC methanolysis reaction (130 °C, 3 h) is shown in Fig. 6c and d. The degree of PC conversion did not change significantly after two cycles of depolymerisation catalysed by ZIF-8 and MOF-5-ED. Conversion remained at 95.8 and 91.0 % for both materials. The efficiency of BPA recovery remained at the level of approx. 92.0 % for ZIF-8 after two cycles. However, after the third reaction, a decrease in yield to 72.2 % was recorded. It implies some level of deactivation of the catalyst [51]. BPA yield dropped from 99.2 % to 67.2 % after the third cycle when MOF-5-ED catalysed reaction. For pristine MOF-5, a considerable

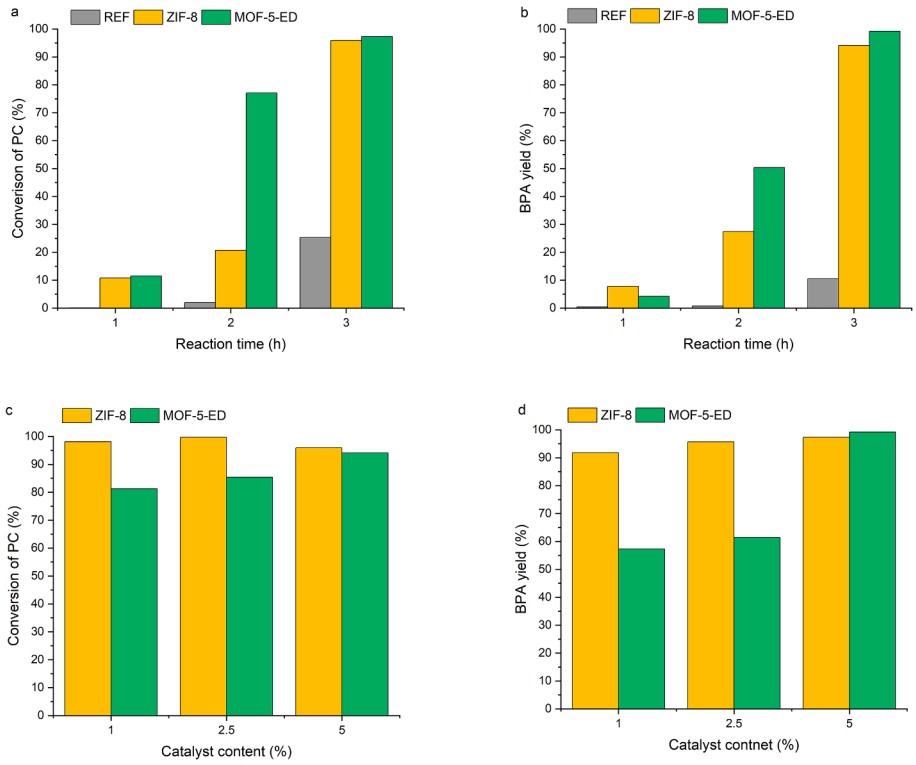

Fig. 5. A, b) influence of the reaction time (1, 2, 3 h) on the PC recycling efficiency. Conditions: T=130 °C, cat. = 5 %. c, d) influence of catalyst concentration (1, 2.5, 5 %) on the PC recycling efficiency. Conditions: T=130 °C, t = 3h.

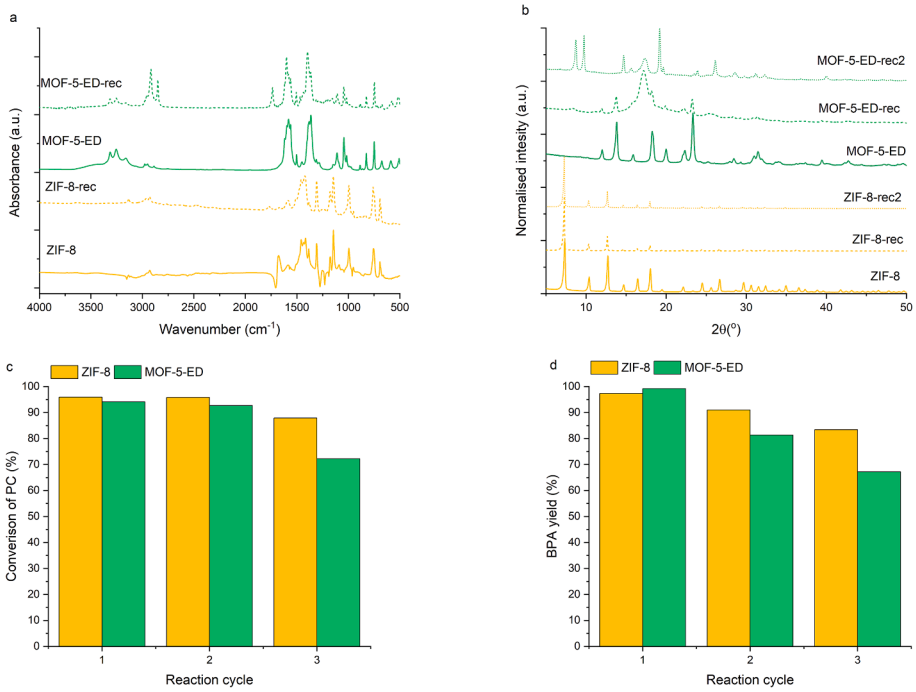

Fig. 6. Characterisation of MOFs before (ZIF-8 and MOF-5-ED) and after recovery (ZIF-8-rec and MOF-5-ED-rec): a) FTIR, b) XRD. Conversion of PC (c) and BPA yield (d) in 1st, 2nd and 3rd reaction cycle, conditions: T=130 °C, cat. = 5 %, t = 3h.

decrease in monomer yield from 34.5 % to 6.6 % was observed after the second reaction (Table A2). However, the PC conversion remained at similar values. Therefore, it can be presumed that the reduced activity of MOF-5-ED can be related to the loss of the ED active species from MOF during its recovery or partial clogging of the MOF structure. Additionally, considering that the active species of ED are grafted onto CUSs via coordination, the leaching in the polar medium methanol after several recycles is likely [22]. Furthermore, the effects of mass transfer limitations on the transesterification reaction suggest that the reaction is partially mass transfer-dependent in the pore system of MOF catalysts.

4. Conclusions

In conclusion, this study explored the potential use of pristine metal–organic frameworks and MOF modified through post-synthetic modification as catalysts for the depolymerisation of polycarbonate through methanolysis.

All applied MOF-based catalysts (UiO-66-NH_2, MAF-6, ZIF-8) showed catalytic activity towards selective cleavage ester bonds in the polymer backbone to its monomers, achieving 49, 89 and 94 % of PC conversion, respectively. Increasing the reaction temperature consistently enhanced PC conversion and BPA yield across all catalysts, with significant improvements noted at 130 °C. The better performance of ZIF-8 and MAF-6 is attributed to their basic active sites and favourable morphologies, while UiO-66-NH_2 lower yields are likely due to restricted mass transfer and less exposed active sites. Additionally, ZIF-8 demonstrated high efficiency in larger-scale reaction and with post-consumer waste, indicating the practical applicability of MOF-based catalysts for PC recycling.

The study also examined the post-synthetic modification of MOF-5 with ethylenediamine (resulting in MOF-5-ED), significantly enhancing its catalytic performance. Structural characterisation by FTIR, XRD analyses confirmed the successful grafting of ED onto MOF-5, maintaining its crystallinity and introducing basic sites that improved catalytic activity. This modification resulted in increasing the PC conversion from ca. 17 to 97 %.

The highest depolymerisation degree was achieved in reactions catalysed by ZIF-8, MAF-6 and MOF-5-ED. The type of basic sites within the MOF structure greatly influenced PC depolymerisation, with an increasing order of efficiency: terephthalic acid < amine terephthalic acid < imidazole < ethylenediamine grafted onto terephthalic acid. The optimal reaction conditions were found to be: 130 °C, 3 h and 5 wt% catalyst loading, preferably using ZIF-8 or MOF-5-ED.

Moreover, the recovery and reusability of MOF catalysts (particularly ZIF-8 and MOF-5-ED) up to three cycles demonstrate their potential for practical application in chemical recycling. Although some decrease in BPA yield was observed after the third cycle, the conversion rates remained high. The decline in activity over successive cycles was linked to potential deactivation and partial clogging of the MOF structure by degradation products, warranting further investigation.

Future research should focus on further PSM strategies or exploring other MOF structures and enhancing the long-term stability of these catalysts over successive reaction cycles to address the observed deactivation. It would be interesting to explore other type of waste, including mixed plastics and coloured waste. Overall, this research opens up new perspectives on the PSM of MOFs and generally on the rational design of MOF-derived solid base catalysts for plastics recycling.

CRediT authorship contribution statement

Patrycja Jutrzenka Trzebiatowska: Writing – review & editing, Writing – original draft, Supervision, Project administration, Methodology, Investigation, Funding acquisition, Formal analysis, Data curation, Conceptualization. **Zofia Maramorosz:** Investigation, Formal analysis, Data curation. **Mateusz A. Baluk:** Writing – review & editing, Investigation, Formal analysis. **Maria Gazda:** Writing – review & editing, Resources, Data curation. **Arantxa Eceiza:** Writing – review & editing, Resources. **Adriana Zaleska-Medynska:** Supervision, Resources, Data curation.

Declaration of competing interest

The authors declare that they have no known competing financial interests or personal relationships that could have appeared to influence the work reported in this paper.

Data availability

The data that support the findings of this study are openly available in RepOD at https://doi.org/10.18150/THAKVK.

Acknowledgments

This work was founded by the National Science Centre, Poland (Narodowe Centrum Nauki, NCN) within the scope of project No. 2021/40/C/ST4/00096.

Appendix A. Supplementary data

Supplementary data to this article can be found online at https://doi.org/10.1016/j.apsusc.2024.160894.

References

[1] I.S. Lase, D. Tonini, D. Caro, P.F. Albizzati, J. Cristóbal, M. Roosen, M. Kusenberg, K. Ragaert, K.M. Van Geem, J. Dewulf, S. De Meester, How much can chemical recycling contribute to plastic waste recycling in Europe? An assessment using material flow analysis modeling, Resour Conserv Recycl 192 (2023) 106916 https://doi.org/10.1016/j.resconrec.2023.106916.

[2] J. Datta, P. Kopczyńska, From polymer waste to potential main industrial products: Actual state of recycling and recovering, Crit Rev Environ Sci Technol 46 (2016) 905–946. doi: 10.1080/10643389.2016.1180227.

[3] I. Vollmer, M.J.F. Jenks, M.C.P. Roelands, R.J. White, T. van Harmelen, P. de Wild, G.P. van der Laan, F. Meirer, J.T.F. Keurentjes, B.M. Weckhuysen, Beyond mechanical recycling: giving new life to plastic waste, Angew Chem Int Ed 59 (2020) 15402–15423, https://doi.org/10.1002/anie.201915651.

[4] R.A. Clark, M.P. Shaver, Depolymerization within a Circular Plastics System, Chem Rev 124 (2024) 2617–2650, https://doi.org/10.1021/acs.chemrev.3c00739.

[5] Statista Research Department, Demand for polycarbonates worldwide from 2011 to 2022, Https://Www.Statista.Com/Statistics/750965/Polycarbonates-Demand-Worldwide/ (2023).

[6] J.W. Gooch, Polycarbonate resin (PC) Encyclopedic Dictionary of Polymers, Springer, New York, NY, 2007, pp. 742–743, https://doi.org/10.1007/978-0-387-30160-0_8858.

[7] R. Singh, S. Shahi, Geetanjali, chemical degradation of Poly(bisphenol A carbonate) waste materials: a review, ChemistrySelect 3 (2018) 11957–11962, https://doi.org/10.1002/slct.201802577.

[8] I.A. Kawa Akbar Masood, Q. Fatima, S.A. Mir, H. Jeelani, S. Manzoor, F. Rashid, Endocrine disrupting chemical Bisphenol A and its potential effects on female health, Diabetes Metab Syndr 15 (2021) 803–811, https://doi.org/10.1016/j.dsx.2021.03.0311.

[9] J.G. Kim, Chemical recycling of poly(bisphenol A carbonate), Polym Chem 11 (2020) 4830–4849, https://doi.org/10.1039/c9py01927h.

[10] E.V. Antonakou, D.S. Achilias, Recent advances in polycarbonate recycling: a review of degradation methods and their mechanisms, Waste Biomass Valorization 4 (2013) 9–21, https://doi.org/10.1007/s12649-012-9159-x.

[11] E.A. Gilbert, M.L. Polo, J.M. Maffi, J.F. Guastavino, S.E. Vaillard, D.A. Estenoz, The organic chemistry behind the recycling of poly(bisphenol-A carbonate) for the preparation of chemical precursors: a review, J Polym Sci 60 (2022) 3284–3317, https://doi.org/10.1002/pol.20220119.

[12] Y. Liu, X.B. Lu, Chemical recycling to monomers: Industrial Bisphenol-A-Polycarbonates to novel aliphatic polycarbonate materials, J Polym Sci 60 (2022) 3256–3268, https://doi.org/10.1002/pol.20220118.

[13] D. Parida, A. Aerts, K. Vanbroekhoven, M. Van Dael, H. Mitta, L. Li, W. Eevers, K. M. Van Geem, E. Feghali, K. Elst, Monomer recycling of polyethylene terephthalate, polycarbonate and polyethers: scalable processes to achieve high carbon circularity, Prog Polym Sci 149 (2024) 101783, https://doi.org/10.1016/j.progpolymsci.2023.101783.

[14] Q. Liu, S. Liu, Y. Lv, P. Hu, Y. Huang, M. Kong, G. Li, Atomic-scale insight into the pyrolysis of polycarbonate by ReaxFF-based reactive molecular dynamics simulation, Fuel 287 (2021) 119484, https://doi.org/10.1016/j.fuel.2020.119484.

[15] P.A. Krisbiantoro, M. Sato, T.M. Lin, Y.C. Chang, T.Y. Peng, Y.C. Wu, W. Liao, Y. Kamiya, R. Otomo, K.C.W. Wu, Low-Temperature Methanolysis of polycarbonate over solid base sodium aluminate, Langmuir 40 (2024) 5338–5347, https://doi.org/10.1021/acs.langmuir.3c03799.

[16] E. Quaranta, C.C. Minischetti, G. Tartaro, Chemical Recycling of Poly(bisphenol A carbonate) by glycolysis under 1,8-diazabicyclo[5.4.0]undec-7-ene Catalysis, ACS Omega 3 (2018) 7261–7268, https://doi.org/10.1021/acsomega.8b01123.

[17] G. Grause, N. Tsukada, W.J. Hall, T. Kameda, P.T. Williams, T. Yoshioka, High-value products from the catalytic hydrolysis of polycarbonate waste, Polym J 42 (2010) 438–442, https://doi.org/10.1038/pj.2010.21.

[18] W. Huang, H. Wang, X. Zhu, D. Yang, S. Yu, F. Liu, X. Song, Highly efficient application of Mg/Al layered double oxides catalysts in the methanolysis of polycarbonate, Appl Clay Sci 202 (2021) 105986, https://doi.org/10.1016/j.clay.2021.105986.

[19] Y. Zhao, H. Jiang, S. Xue, M. Liu, F. Liu, S. Yu, Structures of alkaline earth metal oxides supported on MCF and the enhanced catalytic performance for methanolysis

of polycarbonate, Solid State Sci 107 (2020), https://doi.org/10.1016/j.solidstatesciences.2020.106317.
[20] X. Song, W. Hu, W. Huang, H. Wang, S. Yan, S. Yu, F. Liu, Methanolysis of polycarbonate into valuable product bisphenol A using choline chloride-based deep eutectic solvents as highly active catalysts, Chem Eng J 388 (2020) 124324, https://doi.org/10.1016/j.cej.2020.124324.
[21] F. Iannone, M. Casiello, A. Monopoli, P. Cotugno, M.C. Sportelli, R.A. Picca, N. Cioffi, M.M. Dell'Anna, A. Nacci, Ionic liquids/ZnO nanoparticles as recyclable catalyst for polycarbonate depolymerization, J Mol Catal A Chem 426 (2017) 107–116, https://doi.org/10.1016/j.molcata.2016.11.006.
[22] Y. Lin, C. Kong, L. Chen, Amine-functionalized metal-organic frameworks: Structure, synthesis and applications, RSC Adv 6 (2016) 32598–32614, https://doi.org/10.1039/c6ra01536k.
[23] T.F. Mastropietro, Metal-organic frameworks and Plastic: an emerging synergic partnership, Sci Technol Adv Mater 24 (2023) 2189890, https://doi.org/10.1080/14686996.2023.2189890.
[24] Q. Suo, J. Zi, Z. Bai, S. Qi, The Glycolysis of Poly(ethylene terephthalate) promoted by metal organic framework (MOF) catalysts, Catal Letters 147 (2017) 240–252, https://doi.org/10.1007/s10562-016-1897-0.
[25] M.A. Baluk, P. Jutrzenka Trzebiatowska, A. Pieczyńska, D. Makowski, M. Kroczewska, J. Łuczak, A. Zaleska-Medynska, A new strategy for PET depolymerization: application of bimetallic MOF-74 as a selective catalyst, J Environ Manage 363 (2024) 121360, https://doi.org/10.1016/j.jenvman.2024.121360.
[26] T. Wang, C. Shen, G. Yu, X. Chen, Fabrication of magnetic bimetallic Co–Zn based zeolitic imidazolate frameworks composites as catalyst of glycolysis of mixed plastic, Fuel 304 (2021) 121397, https://doi.org/10.1016/j.fuel.2021.121397.
[27] R. Fang, A. Dhakshinamoorthy, Y. Li, H. Garcia, Metal organic frameworks for biomass conversion, Chem Soc Rev 49 (2020) 3638–3687, https://doi.org/10.1039/d0cs00070a.
[28] Q. Wang, D. Astruc, State of the Art and Prospects in Metal-Organic Framework (MOF)-Based and MOF-Derived Nanocatalysis, Chem Rev 120 (2020) 1438–1511, https://doi.org/10.1021/acs.chemrev.9b00223.
[29] V. Pascanu, G. González Miera, A.K. Inge, B. Martín-Matute, Metal-Organic frameworks as catalysts for organic synthesis: a critical perspective, J Am Chem Soc 141 (2019) 7223–7234, https://doi.org/10.1021/jacs.9b00733.
[30] C. Xu, R. Fang, R. Luque, L. Chen, Y. Li, Functional metal–organic frameworks for catalytic applications, Coord Chem Rev 388 (2019) 268–292, https://doi.org/10.1016/j.ccr.2019.03.005.
[31] A. Amiri, F. Ghaemi, B. Maleki, Hybrid nanocomposites prepared from a metal-organic framework of type MOF-199(Cu) and graphene or fullerene as sorbents for dispersive solid phase extraction of polycyclic aromatic hydrocarbons, Microchim Acta 186 (2019) 1–8, https://doi.org/10.1007/s00604-019-3246-7.
[32] M.N. Timofeeva, V.N. Panchenko, S.H. Jhung, Insights into the Structure–Property–Activity relationship of zeolitic imidazolate frameworks for acid-base catalysis, Int J Mol Sci 24 (2023) 4370, https://doi.org/10.3390/ijms24054370.
[33] L. Zhu, X.Q. Liu, H.L. Jiang, L.B. Sun, Metal-Organic frameworks for heterogeneous basic catalysis, Chem Rev 117 (2017) 8129–8176, https://doi.org/10.1021/acs.chemrev.7b00091.
[34] A. Schaate, P. Roy, A. Godt, J. Lippke, F. Waltz, M. Wiebcke, P. Behrens, Modulated synthesis of Zr-based metal-organic frameworks: From nano to single crystals, Chem Eur J 17 (2011) 6643–6651, https://doi.org/10.1002/chem.201003211.
[35] X. Yang, Z. Wen, Z. Wu, X. Luo, Synthesis of ZnO/ZIF-8 hybrid photocatalysts derived from ZIF-8 with enhanced photocatalytic activity, Inorg Chem Front 5 (2018) 687–693, https://doi.org/10.1039/c7qi00752c.
[36] R.X. Yang, Y.T. Bieh, C.H. Chen, C.Y. Hsu, Y. Kato, H. Yamamoto, C.K. Tsung, K.C. W. Wu, Heterogeneous Metal Azolate Framework-6 (MAF-6) catalysts with high zinc density for enhanced polyethylene terephthalate (PET) conversion, ACS Sustain Chem Eng 9 (2021) 6541–6550, https://doi.org/10.1021/acssuschemeng.0c08012.
[37] J. Chen, R. Liu, H. Gao, L. Chen, D. Ye, Amine-functionalized metal-organic frameworks for the transesterification of triglycerides, J Mater Chem A Mater 2 (2014) 7205–7213, https://doi.org/10.1039/c4ta00253a.
[38] M. Aghajanzadeh, M. Zamani, H. Molavi, H. Khieri Manjili, H. Danafar, A. Shojaei, Preparation of metal-organic frameworks UiO-66 for adsorptive removal of methotrexate from aqueous solution, J Inorg Organomet Polym Mater 28 (2018) 177–186, https://doi.org/10.1007/s10904-017-0709-3.
[39] P. Guan, C. Ren, H. Shan, D. Cai, P. Zhao, D. Ma, P. Qin, S. Li, Z. Si, Boosting the pervaporation performance of PDMS membrane for 1-butanol by MAF-6, Colloid Polym Sci 299 (2021) 1459–1468, https://doi.org/10.1007/s00396-021-04873-y.
[40] H. Kaur, G.C. Mohanta, V. Gupta, D. Kukkar, S. Tyagi, Synthesis and characterization of ZIF-8 nanoparticles for controlled release of 6-mercaptopurine drug, J Drug Deliv Sci Technol 41 (2017) 106–112, https://doi.org/10.1016/j.jddst.2017.07.004.
[41] C.L. Luu, T.T. Van Nguyen, T. Nguyen, T.C. Hoang, Synthesis, characterization and adsorption ability of UiO-66-NH2, Adv Nat Sci Nanosci Nanotechnol 6 (2015) 025004, https://doi.org/10.1088/2043-6262/6/2/025004.
[42] K. Užarević, T.C. Wang, S.Y. Moon, A.M. Fidelli, J.T. Hupp, O.K. Farha, T. Friščić, Mechanochemical and solvent-free assembly of zirconium-based metal-organic frameworks, Chem Commun 52 (2016) 2133–2136, https://doi.org/10.1039/c5cc08972g.
[43] Y.N. Wu, M. Zhou, B. Zhang, B. Wu, J. Li, J. Qiao, X. Guan, F. Li, Amino acid assisted templating synthesis of hierarchical zeolitic imidazolate framework-8 for efficient arsenate removal, Nanoscale 6 (2014) 1105–1112, https://doi.org/10.1039/c3nr04390h.
[44] T. Stassin, I. Stassen, J. Marreiros, A.J. Cruz, R. Verbeke, M. Tu, H. Reinsch, M. Dickmann, W. Egger, I.F.J. Vankelecom, D.E. De Vos, R. Ameloot, Solvent-free powder synthesis and MOF-CVD thin films of the large-pore metal-organic framework MAF-6, Chem Mater 32 (2020) 1784–1793, https://doi.org/10.1021/acs.chemmater.9b03807.
[45] M.N. Timofeeva, I.A. Lukoyanov, V.N. Panchenko, B.N. Bhadra, E.Y. Gerasimov, S. H. Jhung, Effect of MAF-6 crystal size on its physicochemical and catalytic properties in the cycloaddition of CO_2 to propylene oxide, Catalysts 11 (2021) 1061, https://doi.org/10.3390/catal11091061.
[46] A. Dhakshinamoorthy, A. Santiago-Portillo, A.M. Asiri, H. Garcia, Engineering UiO-66 metal organic framework for heterogeneous catalysis, ChemCatChem 11 (2019) 899–923, https://doi.org/10.1002/cctc.201801452.
[47] S. Ibrar, E.O. Ojegu, O.B. Odia, I.L. Ikhioya, S. Afzal, M. Oneeb, I. Ahmad, Assessing high-performance energy storage of the synthesized ZIF-8 and ZIF-67, J Appl Organomet Chem 3 (2023) 294–307, https://doi.org/10.48309/jaoc.2023.421600.1128.
[48] S. Bhattacharjee, M.S. Jang, H.J. Kwon, W.S. Ahn, Zeolitic Imidazolate frameworks: synthesis, functionalization, and catalytic/adsorption applications, Catal Surv Asia 18 (2014) 101–127, https://doi.org/10.1007/s10563-014-9169-8.
[49] Y. Wu, X. Wang, K.O. Kirlikovali, X. Gong, A. Atilgan, K. Ma, N.M. Schweitzer, N. C. Gianneschi, Z. Li, X. Zhang, O.K. Farha, Catalytic degradation of polyethylene terephthalate using a phase-transitional zirconium-based metal-organic framework, Angew Chem Int Ed 61 (2022) e202117528.
[50] J. McMurry, Basicity of amines, in: Organic Chemistry: A Tenth Edition, OpenStax, 2023.
[51] A. Herbst, C. Janiak, MOF catalysts in biomass upgrading towards value-added fine chemicals, CrstEngComm 19 (2017) 4092–4117, https://doi.org/10.1039/c6ce01782g.
[52] D. Kim, B.K. Kim, Y. Cho, M. Han, B.S. Kim, Kinetics of polycarbonate methanolysis by a consecutive reaction model, Ind Eng Chem Res 48 (2009) 6591–6599, https://doi.org/10.1021/ie801893v.
[53] L. Desidery, S. Chaemcheun, M. Yusubov, F. Verpoort, Di-methyl carbonate transesterification with EtOH over MOFs: basicity and synergic effect of basic and acid active sites, Catal Commun 104 (2018) 82–85, https://doi.org/10.1016/j.catcom.2017.10.022.
[54] C.H. Wu, L.Y. Chen, R.J. Jeng, S.A. Dai, 100% Atom-Economy efficiency of recycling polycarbonate into versatile intermediates, ACS Sustain Chem Eng 6 (2018) 8964–8975, https://doi.org/10.1021/acssuschemeng.8b01326.
[55] C. Alberti, S. Enthaler, Depolymerization of end-of-life poly(bisphenol A carbonate) via alkali-metal-halide-catalyzed methanolysis, Asian, J Org Chem 9 (2020) 359–363, https://doi.org/10.1002/ajoc.201900242.
[56] I. Olazabal, E. Luna, S. De Meester, C. Jehanno, H. Sardon, Upcycling of BPA-PC into trimethylene carbonate by solvent assisted organocatalysed depolymerisation, Polym Chem 14 (2023) 2299–2307, https://doi.org/10.1039/d3py00441d.
[57] F. Liu, Y. Xiao, X. Sun, G. Qin, X. Song, Y. Liu, Synergistic catalysis over hollow CeO2-CaO-ZrO2 nanostructure for polycarbonate methanolysis with methanol, Chem Eng J 369 (2019) 205–214, https://doi.org/10.1016/j.cej.2019.03.048.
[58] Z. Fehér, R. Németh, J. Kiss, B. Balterer, K. Verebélyi, B. Iván, J. Kupai, A silica-supported organocatalyst for polycarbonate methanolysis under mild and economic conditions, Chem Eng J 485 (2024) 149832, https://doi.org/10.1016/j.cej.2024.149832.
[59] Y. Zhao, H. Jiang, S. Xue, M. Liu, F. Liu, S. Yu, Structures of alkaline earth metal oxides supported on MCF and the enhanced catalytic performance for methanolysis of polycarbonate, Solid State Sci 107 (2020) 106317, https://doi.org/10.1016/j.solidstatesciences.2020.106317.
[60] Y. Yang, C. Wang, F. Liu, X. Sun, G. Qin, Y. Liu, J. Gao, Mesoporous electronegative nanocomposites of SBA-15 with CaO–CeO 2 for polycarbonate depolymerization, J Mater Sci 54 (2019) 9442–9455, https://doi.org/10.1007/s10853-019-03560-2.
[61] Y.Y. Liu, G.H. Qin, X.Y. Song, J.W. Ding, F.S. Liu, S.T. Yu, X.P. Ge, Mesoporous alumina modified calcium catalyst for alcoholysis of polycarbonate, J Taiwan Inst Chem Eng 86 (2018) 222–229, https://doi.org/10.1016/j.jtice.2018.02.028.
[62] F. Liu, Z. Li, S. Yu, X. Cui, X. Ge, Environmentally benign methanolysis of polycarbonate to recover bisphenol A and dimethyl carbonate in ionic liquids, J Hazard Mater 174 (2010) 872–875, https://doi.org/10.1016/j.jhazmat.2009.09.007.
[63] K.K. Gangu, S. Maddila, S.B. Jonnalagadda, The pioneering role of metal-organic framework-5 in ever-growing contemporary applications - a review, RSC Adv 12 (2022) 14282–14298, https://doi.org/10.1039/d2ra01505f.
[64] M.N. Kajama, Hydrogen permeation using nanostructured silica membranes, in: Sustainable Development and Planning VII, WIT Press, 2015, pp. 447–456, https://doi.org/10.2495/sdp150381.
[65] Y.K. Hwang, D.Y. Hong, J.S. Chang, S.H. Jhung, Y.K. Seo, J. Kim, A. Vimont, M. Daturi, C. Serre, G. Férey, Amine grafting on coordinatively unsaturated metal centers of MOFs: consequences for catalysis and metal encapsulation, Angew Chem Int Ed 47 (2008) 4144–4148, https://doi.org/10.1002/anie.200705998.